UNIVERSITY OF TWENTE.

TACTILE SPATIAL ATTENTION MODULATES ALPHA-MU & BETA BAND ACTIVITY IN PRE-FRONTAL & SOMATOSENSORY CORTEX

MASTER THESIS HUMAN FACTORS & ENGINEERING PSYCHOLOGY

Date: 19/10/2022

Author: Max Weigand - s1848496 – m.k.weigand@student.utwente.nl
1. Supervisor: Dr. Rob van der Lubbe – r.h.j.vanderlubbe@utwente.nl
2. Supervisor: Dr. Russell Chan – r.w.chan@utwente.nl

Table of Content

Abstract

The goal of the present study was to investigate whether there is a difference in functional connectivity between the prefrontal- and primary somatosensory cortex whilst tactile spatial attention is held (sustained) compared to when being interrupted (transient). This was done in order to see whether there is a difference in terms of how strongly the aforementioned brain regions are coupled, indicating a possible advantage of held attention over interrupted attention. Using a pre-recorded dataset, a sensor level-connectivity analysis was conducted within the alpha-mu (8-13Hz) and beta (14-30Hz) to determine possible differences between both conditions in terms of connectivity strength of aforementioned, a-priori chosen cortical regions. Results suggest no clear difference between the two conditions as well as no clear difference in terms of measured activity contralateral vs. ipsilateral to the attended side. Considering previous research on this topic, it was suggested that design issues of the present study might have blurred the effects.

1. Introduction

1.1 Rationale of the Present Study

Attention as a cognitive control, helping us to perceive targeted stimuli, is a broad topic that has been researched in various studies. It was discovered that attentional orienting modulated cortical activity, in turn affecting the processing of subsequently presented stimuli (Wright et al., 2018). For example, Van der Lubbe et al. (2017) examined the effects of sustained and transient tactile spatial attention with regard to nociceptive stimuli processing. In their study, Van der Lubbe et al. (2017) discovered that certain electrodes measured larger frequency oscillations over different cortical regions whilst tactile spatial attention was sustained compared to transient tactile attention, supporting the assumption that held tactile attention increased the efficiency of following stimuli processing.

However, some underlying mechanisms in terms of neuronal activity whilst tactile spatial attention is exercised are still left open for research. One such mechanism is the coupling of cognitive areas whilst tactile spatial attention is constantly being exercised compared to when being interrupted. To examine whether coupled cognitive areas differ in terms of connectivity strength when tactile spatial attention is held compared to when it is being interrupted is interesting as this could provide further insight regarding not only which cortical areas are affected but also clarify relationships between those areas. This, in turn, could further demonstrate the potential for using brain network metrics as biomarkers for predicting task performance (Dai et al., 2017). For example, if a stronger connectivity were to be discovered whilst exercising sustained tactile spatial attention, it could further strengthen the assumption of Van der Lubbe et al. (2017), that sustained tactile attention increases the efficiency of the following processing of stimuli. Additionally, this could, for example, provide further insight to compare neuronal activity of non-clinical subjects with neuronal activity of people suffering from actual attentional-disruptive disorders like attention-deficit/hyperactivity disorder (ADHD). Regarding this topic, Tomasi and Volkow (2012) observed lower functional connectivity between cortical areas associated with attention when researching children with ADHD compared to regular developing children.

Thus, the goal of the present study was to use the pre-recorded dataset of Van der Lubbe et al. (2017) to further examine possible differences between the two tactile spatial attention conditions (sustained vs. transient) in terms of functional connectivity. This type of analysis is used to describe the interaction between coupled cortical regions expressed through the amount of functional coupling (Eickhoff & Müller, 2015). Of course, in order to perform this analysis, first the respective cortical regions of interest (ROI's) have to be identified.

1.2 Cortical Regions of Interest in Relation to Tactile Spatial Attention

Spatial attention manipulations or 'goal-oriented biasing' appear to be represented by mediating top-down signals observed within higher cortical areas (Pessoa et al., 2003; Van Ede et al., 2010). In the study of Wang et al. (2016), this statement was examined using a visual spatial attention task. The motivation was to test the prevailing model of the sensory cortex being affected by mediating top-down signals originating from the frontal and parietal brain areas (Wang et al., 2016). Throughout the visual spatial attention task, participants had to focus on a screen depicting a symbolic cue in form of either a left- or right- pointing arrow instructing them to direct their attention to a square box on the monitor. After random time delays between 1800ms and 2200ms, the target stimulus or a standard stimulus appeared either inside the attended box or in a square box located on the opposite side. Participants were instructed to press a button in case of a target stimulus appearing. Resulting from this visual spatial attention task, the right frontal eye field (FEF) and right inferior gyrus (IFG) were found to be the main sources exerting top-down control onto the occipital cortex (OC). Moreover, alpha activity was found to be suppressed over the visual areas contralateral to the attended visual field. This finding is supported by the study of Di Russo et al. (2021), which also found prefrontal (PFC) activity with a hemispheric lateralization contralateral to the attended side, to be the locus of the top-down visual attention modulation. However, involvement of prefrontal cortex areas as sources of top-down control does not appear to be limited to a visual spatial attention task.

In the study of Adams et al. (2019), the involvement of the prefrontal cortex (PFC) was tested during sensory selections tasks including visual- and tactile stimuli. Using a continuous theta burst stimulation (cTBS), prefrontal cortex activity was transiently inhibited thereby testing its contribution to modulation of sensory gating. Participants were instructed to either track visual stimuli or give a motor response to tactile stimuli, approximating the amplitude of the stimuli through a graded motor response by squeezing a pressure-sensitive rubber bulb. As a result, P50, N70, P100, and N140 peaks were observed in relation to task relevant tactile stimuli. Particularly, somatosensory evoked N70 peaks were shown to be modulated by task relevance. However, after the use of cTBS any significant difference in somatosensory evoked potentials between task relevant- and irrelevant stimuli were nullified. This demonstrated that early modality-specific changes in cortical somatosensory processing are affected by attentional manipulations as well as that this effect is subserved by activity located in the prefrontal cortex (Adams et al., 2019). Other studies support this finding through experiments demonstrating that patients with prefrontal cortex lesions exhibit signs of decreased attention capacity and increased distractibility (Knight et al., 1989; Yamaguchi & Knight, 1990). Therefore, the present study chose the prefrontal cortex as well as the somatosensory cortex as cortical regions of interest in relation to tactile spatial attention.

After reviewing the involvement of the prefrontal cortex, the somatosensory cortex is looked at in more detail. Eimer and Forster (2003) examined how top-down tactile spatial attention affects the somatosensory cortex. They used sustained and transient attention tasks to examine respective differences between those two conditions in order to investigate when and how tactile spatial attention affects somatosensory processing. Here, event-related potentials (ERPs) were computed in response to mechanical tactile stimuli which were delivered to either the left or right hand. In the sustained spatial attention condition participants had to continuously attend either the left or right hand whereas in the transient spatial attention condition participants had to switch attention between hands in an unpredictable manner. Both conditions showed an enhanced N140 component as well as later negativity for attended stimuli compared to unattended stimuli (Eimer & Forster, 2003). Additionally, only in the sustained spatial attention condition, an antecedent increased contra-lateral negativity near the N80 was detected, while transient attention was emulated by a bilateral positivity over the P100 component. Eimer and Forster (2003) concluded that sustained spatial attention affects tactile processing within the so called ‘primary somatosensory cortex’ (SI) whereas transient spatial attention affects the ‘secondary somatosensory cortex’ (SII) and later stages. These results are partly in line with another study which observed how tactile spatial attention affects power oscillations within the brain (Anderson & Ding, 2011). For this study, again, two conditions were examined, (1) attend & (2) ignore, resulting in contralateral pre-stimulus power decrease for both conditions over electrodes CP3 and CP4 (i.e., somatosensory activity). Similar patterns over the occipital cortex have been observed for visual spatial attention (Rajagovindan & Ding, 2011; Thut et al., 2006).

Informed by the studies discussed above, the somatosensory- and prefrontal cortex are regions of interest (ROI’s) regarding tactile spatial attention related brain regions thought to interact before the actual tactile stimulus onset, i.e. during the orientation phase. Thus, the present study investigated those two ROI’s, that is, the coupling between those two regions as the main research goal.

1.3 Frequency Bands affected by Tactile Spatial Attention

Results of the study of Whitmarsch et al. (2017) suggest that, during the performance of a tactile discrimination task requiring sustained attention, the process of attention significantly suppresses somatosensory alpha oscillations in the range between 8 Hz – 14 Hz. Oscillations of pre-stimulus alpha frequencies in sensory cortex areas were found to determine subsequent performance including tactile detection and discrimination (Haegens et al., 2011; Weisz et al., 2014). A decrease in alpha power in relation to tactile spatial attention was found to mirror an increase of excitability over sensory cortical areas enhancing the processing of (approaching-) stimuli (Eimer & Forster, 2003). An increase in alpha power in relation to spatial attention was found to mirror a decreased excitability over sensory cortical areas like as a potential mechanism to block out externals sensory input thus protecting held information currently stored/processed in the working memory (Jensen & Mazaheri, 2010; Klimesch, 2012; Mathewson et al., 2011). More precisely, it appears that especially higher alpha bands, characterized as ‘mu-rhythm’ (~8 Hz – 13 Hz) over the somatosensory cortex are modulated by tactile spatial attention (Weiss et al., 2018). That is in line with the study of Van der Lubbe et al. (2017), which also examined cortical activity during the orientation phase of sustained and transient tactile attention tasks. These results suggested that modulation concerns inhibition of alpha bands expressed within ipsilateral connections (Van der Lubbe et al., 2017).

However, tactile spatial attention related signals do not seem to be limited to the alpha-mu frequency band. Other studies observed that pre-stimulus beta oscillations (~14 Hz - 30 Hz) are associated with conscious detectability of tactile stimuli (Linkenkaer-Hansen et al., 2004; Palva et al., 2005). In the study of Ede et al. (2010), beta oscillations in the somatosensory cortex related to tactile spatial attention were examined. Here, beta oscillations were investigated in the light of attentive and non-attentive tactile expectations. Based on the results, it was argued that tactile attention is reflected by suppression of beta power originating, at least partly, from the primary somatosensory cortex contralateral to the expected stimulation (Ede et al., 2010). Therefore, beta oscillations seem to be affected by tactile spatial attention as well.

1.4 The Present Study

The main goal of the present study was to examine if, a priori chosen, coupled cortical regions (i.e., prefrontal (AF3/AF4)- & somatosensory cortex (CP3/CP4) show differences in terms of functional connectivity when exercising sustained tactile spatial attention compared to transient tactile spatial attention. The cortical regions were chosen based on previous studies examining similar tactile attention tasks such as Eimer and Forster (2003) or Van der Lubbe et al. (2017). The choice of the respective electrode pairs was made based on the location of these electrodes within the extended 10-20 electrode system (Lotte et al., 2015). Additionally, Anderson and Ding (2011), who also examined activity over the primary somatosensory cortex, chose CP3/CP4 as respective representing region of interest, as electrodes placed over this area measured the largest early evoked activity. Thus, the respective approach was to compare (possible) spatiotemporal overlaps of coupled brain regions of both conditions.

It was expected that, compared to the transient condition, stronger connectivity between PFC (AF3/AF4) and S1 (CP3/CP4) is found within alpha-mu and beta frequency in the sustained condition (in the time interval before the actual tactile stimuli onset). That is because, in the sustained condition, participants were able to constantly focus on either the left- or right- hand side allowing them to focus their attention on one side even before the instruction was presented on the screen. In contrast, during the transient condition, participants had to relocate their tactile attention every trial. Additionally, it is expected that, at least in the sustained attention condition, alpha-mu and beta power oscillations are found within the prefrontal- and primary somatosensory cortex contralateral to the attended hand.

2. Methods

2.1 Participants

For the purpose of the present study, electroencephalographic recordings (EEG) of 17 participants were used (3 male, 14 female, M_{age} = 24.1 years, SD_{age} = 3.5, age range: 20-34 years). From these 17 participants two had to be excluded due to technical and procedural errors during the recording. All participants reported to have normal or corrected-to-normal eyesight and to be free of psychiatric and neurological disorders. Every participant signed an informed consent as well as received a detailed description of the procedure of the recording. Additionally, the 'Medical Ethical Committee of Medisch Spectrum Twente' approved the experimental procedure (NL31474.0044.11/P11-11).

2.2 Materials

To collect the data, Ag/AgCl electrodes mounted on an electro-cap (EasyCap GmbH, Herrsching-Breitbrunn, Germany) were used which recorded EEG data from 61 standard channel positions (i.e., the extended 10-20 system). All electrode impedances were kept below 10 kΩ. Additionally, the vertical and horizontal electrooculogram (vEOG & hEOG) were recorded using bipolar Ag/AgCl electrodes positioned at the outer canthi of both eyes as well as from above and below the left eye. Subsequently, the recorded signals were sent through a 72 channel QuickAmp-amplifier of the Brain Products GmbH *(*Munich, Germany*)*. Two Digitimer DS5 constant current stimulators (Digitimer, Welwyn Garden City, UK) were used to convey electrical stimuli through means of bipolar concentric electrodes. The 'E-Prime Software' (version 2.0) controlled stimulus presentation, response registration, and production of external triggers. Finally, the data was recorded online with an in-built average reference at a sample rate of 500 Hz and an applied 200 Hz low pass filter as well as a 50 Hz notch filter.

To pre-process and analyse the recorded data the MNE-Python software (version 0.22.0) was used including common M/EEG processing algorithms (see Appendix A1). In order to use these code snippets, additional MNE-Python toolboxes had to be installed, namely: (1) Filtering, (2) Independent Component Analysis, (3) Connectivity estimation, and (4) Statistics (Gramfort et al., 2014).

Lastly, the ‘R-Studio’ software was used to conduct the statistical analysis of each recorded electrode connection of interest.

2.3 Design & Procedure

The within-subject, multi-modal electroencephalographic dataset used in the present study was originally reported by Van der Lubbe et al. (2017)[1]. After the participants were told about the purpose of the study, they were equipped with the electro-cap as well as connected to the current simulator using the bipolar concentric electrodes. These selectively activate Aδ-fibers located in the epidermis through means of a small needle which was inserted right under the skin over the median nerves of the right and left forearm (Inui et al., 2002).

[1] https://easy.dans.knaw.nl/ui/datasets/id/easy-dataset:76135

Figure 1

Diagram showing a trail example used in the original study with one possible visual cue depiction (out of two) and a following visualisation of the nociceptive stimuli onset (little flash) as well as the respective timeline on the right (Van der Lubbe et al., 2017)

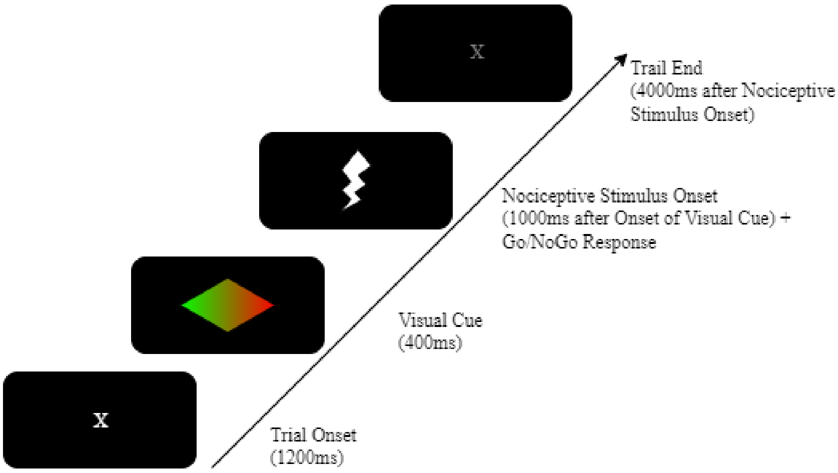

The build-up of each trial began with a white fixation cross (0.48cm * 0.48cm) shown at the centre of a CRT screen. After 1200ms, the cross was replaced by the visual cue in form of a rhomb (3.62cm * 1.91cm) being presented for 400ms. The rhomb consisted of a red and green triangle with one signalling the to-be- attended side which, in turn, depended on the relevant cue colour within that specific block. 1000ms after the visual cue onset, a nociceptive stimulus was delivered at the participants forearm, left or right, one thousand milliseconds after the visual cue onset. Each trial ended 4000 ms after the nociceptive stimulus onset indicated by the white fixation cross turning grey.

In total, the experiment consisted of four blocks with 96 trials respectively and an additional short block of 16 practice trials being presented before the start of the third block. The blocks were designed in such a way that, in the sustained attention blocks (1 & 3 or 2 & 4, order counterbalanced), the relevant colour was presented on the right side throughout the first half of the block and on the left side throughout the second half or vice versa. On the other hand, the transient attention blocks (2 & 4 or 1 & 3, order counter-balanced) changed the side of the relevant colour randomly each trial.

For the analysis, the pre-recorded raw data was pre-processed and, subsequently, a ‘sensor-level spectral connectivity analysis*’* between the electrode pairs AF3/AF4 and CP3/CP4 was conducted. These a priori chosen electrode pairs were picked based on studies such as Van der Lubbe et al. (2017) which also examined tactile spatial attention representation within cortical areas as well as the electrode location within the extended 10-20 electrode system. That is supported by the study of Anderson and Ding (2011) which also included CP3/CP4 to represent activity over the primary somatosensory cortex as those measured largest early evoked activity. On the other hand, the study of Wang, et al. (2016) chose AF3 as to represent activity over the prefrontal cortex.

2.4 EEG Data – Analysis Pipeline

Firstly, each recording was examined for channels showing irregular noisy signals, flat lines, and frequencies resembling heartbeat or muscle movements. In case of a substantial problem with a channel, meaning that non-cortical originating noise or flat lines continued for more than 40% within the duration of the whole recording, it was marked as bad. Subsequently, bad channels were interpolated, using the ‘spherical spline’ method. This method projects the locations of the marked electrodes onto a unit sphere and interpolates its signal based on surrounding signals of good electrodes (Perrin et al., 1989).

Next, the continuous data was filtered using a band-pass filter with the range of 0.1 Hz to 30 Hz suppressing all frequency components above or below these cut-off values. Subsequently, an ‘Independent Component Analysis’ (ICA) was conducted, using the ‘fastica’ algorithm, in order to exclude components with no cortical origin. Here, previously dedicated EOG channels were used to check the IC components against. In case of matching patterns those respective channels were excluded. Additionally, IC components with patterns resembling heartbeat, muscular movements or deviant signals were manually removed, as well. This resulted in an average of 3.53 excluded components out of 61 per participant (SD = 1.55). For more information how MNE applies ICA, see Appendix A.

Next, transient and sustained nociceptive stimuli onsets were chosen as event markers. Thereof, epochs were formed, ranging from -1250 ms until 0 ms relative to the nociceptive stimulus onset. This covered the time interval from 250 ms before the visual cue onset till the onset of the nociceptive stimuli. Moreover, the first 250 ms of the epoch were indicated as baseline which, however, was not included in the final connectivity analysis described further down. Next, rejection criteria were defined for each channel within the formed epochs to exclude remaining smaller artefacts (maximum peak-to-peak amplitudes: 100μV, minimum peak-to-peak amplitudes: 1μV for interval length of whole epoch).

Lastly, a ‘sensor level spectral connectivity analysis’ was applied to every epoch (minus the baseline) of both conditions. This connectivity analysis was carried out for all relevant conditions. The ‘phase lag index’ –approach (PLI) was used, in order to calculate the connectivity between the respective electrode pairs (AF3/AF4 & CP3/CP4) for frequency bands, mu-alpha and beta. The PLI approach was used as it is a measure of phase synchronization designed to reduce effects of volume conduction by ignoring zero and pi (π) phase differences (Stam et al., 2007). In more detail, the PLI estimates the asymmetry of the distribution of instantaneous phase differences, which are determined by using the Hilbert transformation between two signals (González et al., 2018). The PLI ranges between zero and one with zero indicating phase differences that centre around zero mod π (i.e., no coupling) while values close to one indicate stronger nonzero phase locking (i.e., strong coupling). These phase synchronization metrics are favourable to use for short-duration events to determine the connectivity of two signals across trials (Aydore et al., 2013; Bowyer, 2016). Moreover, for the PLI computations, the connectivity scores were averaged for each frequency band using the 'multitaper spectrum estimation' with seven digital prolate spheroidal sequence (DPSS) -windows (or Slepian windows).

2.5 Statistical Analysis

Lastly, the final statistical analysis was conducted using the R-Studio statistics programme (RStudio Team, 2022). For the analysis a multi-factorial linear model approach was chosen. This decision was made because, in case of the present study, statistical modelling had more advantages as well as higher reliability compared to the ANOVA which was conducted first (Hernandez, 2018). The most relevant advantages in this case were that independent from the sample size different factors or factor combinations could be considered simultaneously. Firstly, this was of advantage considering the low sample size (15) of the present study. Secondly, as the data of both frequency bands, i.e. connectivity values, were computed on a continuous scale (PLI) ranging from zero to one, a normal distribution was unlikely and, in fact, not given. Thus, it was decided that a Beta distribution would be most fitting. That is because a Beta distribution is a continuous distribution modelling variables of values falling inside a finite interval, with the standard Beta distribution using the interval between zero and one (Gupta & Nadarajah, 2004). By applying the computed connectivity values between the electrode pairs, the multi-factorial linear model analysis was used to draw a comparison between the following factors of interest: (1) Attention Condition (Sustained & Transient), (2) Attended Side (Left & Right), and (3) Electrode Pair (AF3-CP3 & AF4-CP4).

3. Results

First, a two-way ANOVA was conducted using a 'Bonferroni' correction as confidence interval adjustment. For this analysis the same factors were used (i.e. Attention Condition, Attended Side, and Electrode Pair). However, none of the respective results indicated a significant interaction between those factors and are thus presented only in the

Appendix. Therefore, only the results of the multi-factorial linear model approach are shown in this results section as this analysis allows for the inclusion of more data. Firstly, a visual representation of the examined electrodes AF3, AF4, CP3, and CP4 is presented in Figure 2. As one can see in Figure 3 and 4, the connectivity values, expressed through a depiction of the means and standard deviations, are close to zero indicating a rather weak connectivity between the respective electrode pairs in both conditions. That is the case for both the alpha-mu and beta frequency band.

Figure 2

Visual representation of locations of the examined electrodes AF3, AF4, CP3, and CP4. The arrows were only added to further the understanding of locations of the electrodes, however, they do ***not*** *act as representatives for the actual computed connectivity values.*

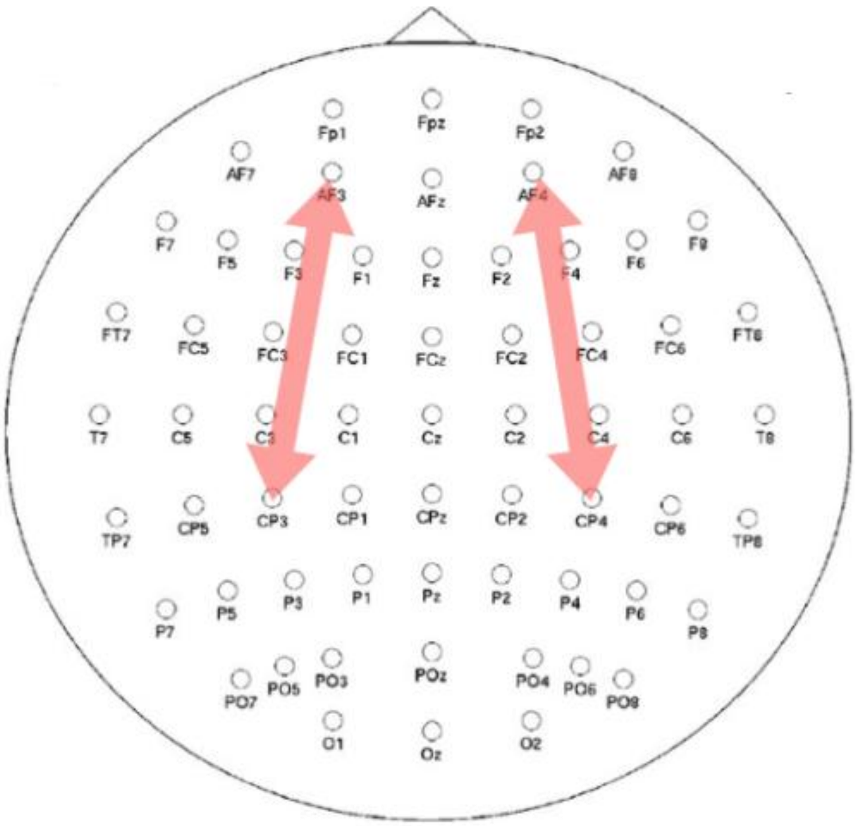

Figure 3

Bar Chart of the Connectivity of each Condition, Attended Side, and Electrode Pair within the ***alpha-mu frequency*** *range. Bars represent the mean connectivity with the respective standard deviation represented by the bars above.*

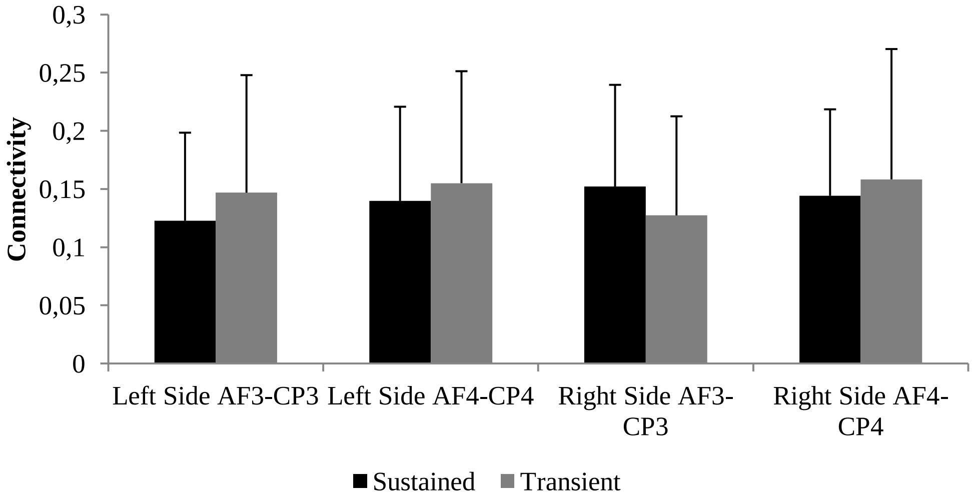

Note. All mean values fall below 0.2 with even standard deviations not reaching a maximum value over 0.3 indicating a low connectivity. Also, against expectations, the sustained condition does not appear to have a stronger connectivity compared to the transient condition.

Figure 4

Bar Chart of the Connectivity of each Condition, Attended Side, and Electrode Pair within the ***beta frequency range****. Bars represent the mean of each connectivity with the respective standard deviation represented by the bars above.*

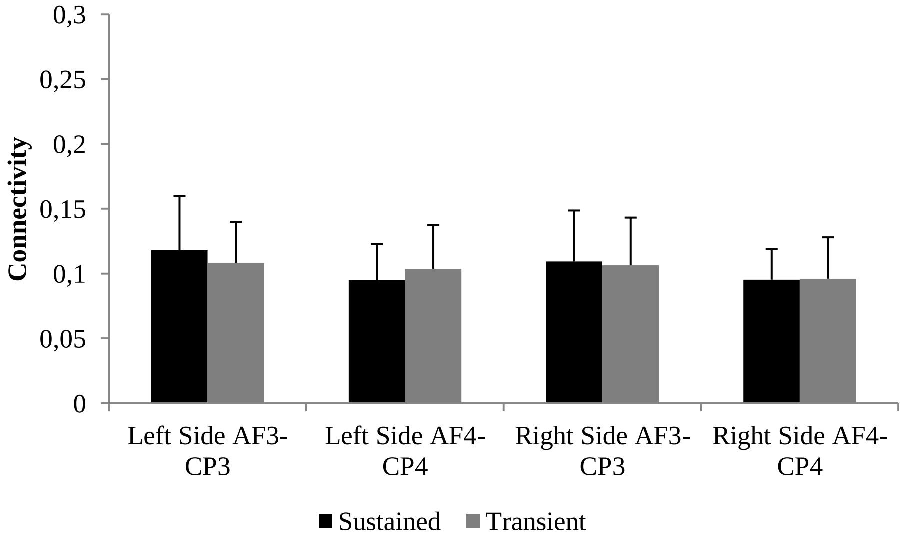

Note. All mean values fall below 0.15 with even standard deviations not reaching a maximum value over 0.2 indicating an even lower connectivity compared to the alpha-mu frequency. Again, against expectations, the sustained condition does not appear to have a stronger connectivity compared to the transient condition.

In order to test if the differences between conditions can be considered substantial a subsequent multi-factorial linear model analysis was conducted for each frequency bands. Additionally, an analysis for the best model fit was conducted, which indicated that the model should include the interactions between factors. The respective graphs can be found in the Appendix. Therefore, the final multi-factorial linear model included the aforementioned factors (Condition, Side, & Electrode Pair) as well as the respective interactions between those factors (Condition x Side, Condition x Electrode Pair, Side x Electrode Pair). The respective model results are shown in the following Table 1 and 2.

Table 1

Outcomes of the multi factorial linear model analysis within the ***alpha-mu frequency band*** *focusing on the electrode pair AF3/4 and CP3/4. With the intercept being the sustained conditions' electrode pair AF3/CP3. Transient condition and right side include both electrode pairs AF3-CP3 and AF4 CP4. The interaction of transient condition and the electrode pair includes both sides and the interaction of the right side and electrode pair AF3-CP3 includes both conditions. All conditions and factors are compared to the intercept. Upper and lower ranges have a confidence interval of 95%.*

	Center	Lower	Upper
Intercept	-1.903	-2.249	-1.592
Transient Condition	0.078	-0.348	0.512
Right Side	0.162	-0.290	0.581
Electrode Pair AF4-CP4	0.091	-0.348	0.521
Transient Condition & Right Side	-0.205	-0.719	0.281
Transient Condition & Electrdoe Pair AF4-CP4	0.062	-0.416	0.549
Right Side & Electrode Pair AF4-CP4	-0.051	-0.529	0.445

Note. These are transformed values, i.e. not the actual connectivity values measured. They are the result of the statistic program (R-studio) adding so called 'dummies' based on the original values in order to compute values on the logit-scale indicating the relation between each other. Transforming them back, however, increases the risk of inaccuracy. No p-values were produced.

Referring back to the means and standard deviations of the connectivity between AF3-CP3 and AF4-CP4 within the alpha-mu frequency band no difference seems present (see Figure 3). The respective model showed that the intercept is with 95% certainty between -2.249 and -1.592, with a centre of -1.903 on the logit scale (Table 1). This indicates that the population mean connectivity is between -2.249 and -1.592 with it most likely being -1.903 on the logit scale for the sustained, attended left side, AF3-CP3 condition. Next, the focus is going to be on relative differences on the logit scale instead of absolute differences on a regular scale as this allows for a somewhat easier and more extensive interpretation.

Regarding Table 1, the two largest differences from the intercept is the interaction between the transient condition and attended right side as well as the attended right side mean. One can say with 95% certainty that the center estimation of the mean connectivity of the interaction between the transient condition and attended right side differs by -0.205 from the intercept which amounts to a difference of 10.77%. As for the second largest difference one can say with 95% certainty that the center estimation of the mean connectivity of the attended right side factor differs by 0.162 from the intercept which equals to 8.51%. On the other hand, referring back to Table 1, one can see that only part of the confidence interval for both, interaction and factor models, are outside of the confidence interval of the intercept. That means that it is likely that the population means between those are not much different. Thus, no definite conclusion can be drawn from these results.

Table 2

*Outcomes of the multi factorial linear model analysis within the **beta frequency band** focusing on the electrode pair AF3/4 and CP3/4. With the intercept being the sustained conditions' electrode pair AF3/CP3. Transient condition and right side include both electrode pairs AF3-CP3 and AF4 CP4. The interaction of transient condition and the electrode pair includes both sides and the interaction of the right side and electrode pair AF3-CP3 includes both conditions. All conditions and factors are compared to the intercept. Upper and lower ranges have a confidence interval of 95%.*

	Center	Lower	Upper
Intercept	-2.041	-2.211	-1.883
Transient Condition	-0.042	-0.257	0.171
Right Side	-0.051	-0.277	0.166
Electrode Pair AF4-CP4	-0.180	-0.409	0.038
Transient Condition & Right Side	-0.030	-0.291	0.228
Transient Condition & Electrode Pair AF4-CP4	0.088	-0.163	0.349
Right Side & Electrode Pair AF4-CP4	0.032	-0.226	0.291

Note. These are transformed values, i.e. not the actual connectivity values measured. They are the result of the statistic program (R-studio) adding so called 'dummies' based on the original values in order to compute values on the logit-scale indicating the relation between each other. Transforming them back, however, would lead to inaccuracy. No p-values were produced.

Considering the means and standard deviations of the connectivity between AF3-CP3 and AF4-CP4 within the beta frequency band, again, no difference seems present (see Figure 4). The respective model showed that the intercept is with 95% certainty between -2.211 and -1.883, with a center of -2.041 on the logit scale (Table 2). This indicates that the mean connectivity is -2.041 on the logit scale for the sustained, attended left side, AF3-CP3 condition. For further interpretation the focus is, again, on relative differences on the logit scale.

Referring back to Table 2, the most substantial difference from the intercept is found for the mean connectivity of electrode pair AF4-CP4 which, with 95% certainty, differs by -0.180 (8.82%). Additionally, again one can see that only part of the confidence interval for the 'electrode pair AF4-CP4' model is outside of the confidence interval of the intercept. Thus, again, no definite conclusion can be drawn from these results.

4. Discussion

The present study focused on the connectivity between brain regions of interest (ROI's) during tactile spatial attention tasks. The goal was to examine possible differences of functional connectivity between a-priori chosen electrode pairs located over the prefrontal- and somatosensory cortex whilst participants exercise sustained tactile spatial attention compared to transient tactile spatial attention. These connectivity differences were examined for the alpha-mu (8-12Hz) frequency- band as results from the original study of this data set suggest that tactile attention modulation concern inhibition of alpha bands (Van der Lubbe et al., 2017). Additionally, connectivity differences were examined for the beta (14-30Hz) frequency band since studies like Ede et al. (2010) also argued, based on their results, that tactile spatial attention is reflected by suppression of beta power. Based on previous research, for example Eimer and Forster (2003), it was expected to find a stronger connectivity between the electrode pairs of AF3/CP3 and AF4/CP4 for the sustained attention condition compared to the transient attention condition within both, alpha-mu and beta frequency bands. Based on the results, however, no clear difference in terms of connectivity strength was found between the two conditions for both, ipsilateral as well as contralateral coupled regions of interest.

One reason for the non-significant results is that individual differences may have blurred effects. Individual alpha peak frequency (IAPF), for example, is one factor that could be considered for this case. Klimesch (1999) defined this term as the maximum power value recorded within the EEG alpha frequency band varying between 7.5 Hz and 12.5 Hz. Higher IAPF has been suggested to mirror the state of cognitive preparedness thus being defined as a measure of cognitive capacity for action/function otherwise referred to “a brain trait or state that sets the stage for optimal cognitive performance” (Angelakis et al., 2004a, p. 889).

This ‘state’, in turn, was further studied to the point that IAPF can be interpreted as a variable indicating intra-individual variability best reflected throughout pre-performance periods similar to the one examined in the present study (Angelakis et al., 2004b, Haegens et al., 2014). Angelakis et al. (2004a), for instance examined one of these intra-individual variabilities with the result that cognitive preparedness, i.e. pre-task IAPF, for non-clinical participants was significantly correlated with the performance of the working memory throughout the first run of the test, however, not on the second run. This led to the conclusion that pre-task IAPF may vary for individuals each reflecting their own level of preparedness to take action. Applying this conclusion of Angelakis et al. (2004a) to the non-significant results of the present study, one could argue that intra-individual variability may have had an impact on the not found significance between the two conditions as fluctuating IAPF’s across participant blurred the possible line between sustained and transient states. Thus, it might be of importance to examine the computed connectivity values of each participant individually instead of averaging multiple participants' data as it has been done in the present study.

Another reason which could have affected the low connectivity found in the present study is the so called 'hemispheric utilization bias'. This term is defined as individual characteristic bias to utilize one cerebral hemisphere over the other (Levy et al., 1983). In terms of spatial attention, each cerebral hemisphere has the capability for directing attention as well as perceptual representation and was proven to be able to operate independently (Arguin et al., 2000; Corballis & Gratton, 2003; Luck et al., 1994). Respectively, each hemispheric attention system appears to possess inhibitory biases striving to direct attention to the contralateral direction with the left hemisphere generally having a more potent bias compared to the right hemisphere (Kinsbourne, 2013). Therefore, the low connectivity values of the present study could be partly explained by this 'hemispheric utilization bias' as, similar to the IAPF, individuals appear to have a inherit preference of using the hemisphere over the other. Thus, again, by averaging those connectivity values, this bias could have led to lower scores than expected.

Another design issue of the present study that could have led to the non-significant results found between the two conditions could be the block order of the present study. As described in the method section, the respective conditions were presented in turns throughout the blocks of the experiment. This could have led to blurred effects between the two conditions. As Angelakis et al. (2004a) pointed out IAPF seems to be correlated with the working memory. Therefore, having a clear cut between conditions instead of the design of the present study, i.e. mixed condition blocks, could have led to a more distinct contrast between the two conditions. That is because when using a clear cut between conditions, participants could have a improved understanding about whether they are expected to hold tactile spatial attention directed to either the left or right side or whether those sides are going to switch throughout the blocks.

Yet another design issue that could have led to such low computed connectivity values could be that participants did not exercise solely tactile spatial attention but also, for example, visual spatial attention. It could be argued that this is the case due to how tactile spatial attention conditions were executed. In some studies, for example Eimer and Forster (2003), eyesight of the participants was prevented through techniques like dimming the light or delivering the tactile stimuli outside of the participants' sight. Thus, the possibility of mixed visual and tactile spatial attention was eliminated and a clear distinction between sustained and transient tactile spatial attention was found. In the present study, however, participants experienced not just tactile- but also visual cues which might possibly explain the low connectivity.

Lastly, the limited number of electrodes included could have been another design issue of the present study. Although, it is rather unlikely that the wrong electrode pairs were chosen, as the choice was made based on previous studies such as Van der Lubbe et al. (2017) which recorded the data used in the present study. However, the inclusion of more electrodes, if not all, in the statistical analyses would be recommendable. For example, in the case of the present study this would have been helpful as one could observe connectivity values of frontal eye field (FEF) electrodes to test possible influence of visual spatial attention. Additionally, one could use collapsed localizers besides the literature-based analysis. Thus, the connectivity for the whole dataset could have been included by collapsing the two conditions in order to select the collapsed localizers (Luck & Gaspelin, 2016). By doing so the highest connectivity between all electrode pairs could have been examined. This, in turn, could have provided more insight into actual behaviour of the participants during the experiment and possibly underlined the idea that more than tactile spatial attention was at work.

In conclusion, there were a number of issues in the present study that could have led to the non-significant results found and thus to the rejection of our assumption that a stronger connectivity between the ROI's would be present for the sustained tactile spatial attention condition compared to the transient tactile spatial attention condition. Thus for future research we recommend, firstly, to make sure that, when examining on sense in particular (i.e. here tactile), to block out all other senses, similar to how the study of Eimer and Forster (2003) in which they covered participants eyes to prevent visual attention. Also it is recommended to look at participants recorded data individually to avoid the IAPF as well as the hemispheric utilization bias. Also it is recommended for future research to have a clear cut between the condition blocks instead of mixing them up as was done by the present study. Lastly, we recommend for future research to collect data of all electrodes instead of using 'only' two electrode pairs in order to examine possible activity from electrodes which were not the initial focus of the study. This, in turn, could help to understand what was actually happening throughout the experiment. Having corrected these issues we would expect that results are more similar to the results of previous research such as Van der Lubbe et al. (2017) or Eimer and Forster (2003).

References

Adams, M. S., Andrew, D., & Staines, W. R. (2019). The contribution of the prefrontal cortex to relevancy-based gating of visual and tactile stimuli. *Experimental Brain Research, 237*(10), 2747-2759. DOI: 10.1007/s00221-019-05633-9

Anderson, K. L. & Ding, M. (2011). Attentional modulation of the somatosensory mu rhythm. *Neuroscience, 180*(), 165-180. DOI: 10.1016/j.neuroscience.2011.02.004

Angelakis, E., Lubar, J:F., Stathopoulou, S., & Kounois, J. (2004a). Peak alpha frequency: an electroencephalographic measure of cognitive preparedness. *Clinical Neurophysiology, 115*(4), 887-897. DOI: 10.1016/j.clinph.2003.11.034

Angelakis, E., Lubar, J. F., & Stathopoulou, S. (2004b). Electroencephalographic peak alpha frequency correlated of cognitive traits. *Neuroscience Letters, 371*(1), 60-63. DOI: 10.1016/j.neulet.2004.08.041

Arguin, M., Lassonde, M., Quattrini, A., Del Pesce, M., Foschi, N., & Papo, I. (2000). Divided visuo-spatial attention systems with total and anterior callosotomy. *Neuropsychologia*, *38*(3), 283-291. DOI: 10.1016/S0028-3932(99)00077-9

Aydore, S., Pantazis, D., & Leahy, R. M. (2013). A note on the phase locking value and its properties. *NeuroImage, 74*(), 231-244. DOI: 10.1016/j.neuroimage.2013.02.008

Bowyer, S. M. (2016): Coherence a measure of the brain networks: Past and Present. *Neuropsychiatric Electrophysiology, 2*(1), 1-12. DOI: 10.1186/s40810-015-0015-7

Corballis, P. M. & Gratton, G. (2003). Independent control of processing strategies for different locations in the visual field. *Biological Psychology, 64*(1-2), 191-209. DOI: 10.1016/S0301-0511(03)00109-1

Dai, Z., Souza, J., Lim, J., Ho, P. M., Chen, Y., Li, J., Thakor, N., Bezerianos, A., & Sun, Y. (2017). EEG cortical connectivity analysis of working memory reveals topological reorganization in theta and alpha bands. *Frontiers in Human Neuroscience, 11*(237). DOI: 10.3389/fnhum.2017.00237

Di Russo, F., Berchicci, M., Bianco, V., Perri, R. L., Pitzalis, S., & Mussini, E. (2021). Modulation of anticipatory visuospatial attention in sustained and transient tasks. *Cortex, 135*(), 1-9. DOI: 10.1016/j.cortex.2020.11.007

Ede, F., Jensen, O., & Maris, E. (2010). Tactile expectation modulates pre-stimulus β-band oscillations in human sensorimotor cortex. *NeuroImage*, *51*(2), 867-876. DOI: 10.1016/j.neuroimage.2010.02.053

Eickhoff, S. B. & Müller, V. I. (2015). Functional Connectivity. *Brain Mapping, 2*(), 187-201. DOI: 10.1016/B978-0-12-397025-1.00212-8

Eimer, M. & Forster, B. (2003). Modulations of early somatosensory ERP components by transient and sustained spatial attention. *Experimental Brain Research, 151*(1), 24-31. DOI: 10.1007/s00221-003-1437-1

González, G. F., Smit, D. J. A., van der Molen, M. J. W., Tijms, J., Stam, C. J., de Geus, E. J. C., & van der Molen, M. W. (2018). EEG Resting State Functional Connectivity in Adult Dyslexics using Phase Lag Index and Graph Analysis. *Frontiers in Human Neuroscience, 12*(341), 1-12. DOI: 10.3389/fnhum.2018.00341

Gramfort, A., Luessi, M., Larson, E., Engemann, D. A., Strohmeier, D., Brodbeck, C., Parkkonen, L., & Hämäläinen, M. S. (2014). MNE software for processing MEG and EEG data. *NeuroImage, 86*(), 446-460. DOI: 10.1016/j.neuroimage.2013.10.027

Gupta, A. K. & Nadarajah, S. (2004). *Handbook of Beta Distribution and Its Applications.* CRC Press. DOI: 10.1201/9781482276596

Haegens, S., Cousijn, H., Wallis, G., Harrison, P. J., & Nobre, A. C. (2014). Inter- and intra-individual variability in alpha peak frequency. *NeuroImage, 92*(), 46-55. DOI: 10.1016/j.neuroimage.2014.01.049

Haegens, S., Händel, B. F., & Jensen, O. (2011). Top-Down Controlled Alpha Band Activity in Somatosensory Areas Determines Behavioral Performance in a Discrimination Task. *Journal of Neuroscience, 31*(14), 5197-5204. DOI: 10.1523/JNEUROSCI.5199-10.2011

Hernandez, H. (2018). Statistical Modeling and Analysis of Experiments without ANOVA. https://doi.org/10.13140/RG.2.2.21499.00803.

Inui, K., Tran, T. D., Hoshiyama, M., & Kakigi, R. (2002). Preferential stimulation of Aδ fibers by intra-epidermal needle electrode in humans. *Pain, 96*(3), 247-252. DOI: 10.1016/S0304-3959(01)00453-5

Jensen, O. & Mazaheri, A. (2010). Shaping functional architecture by oscillatory alpha activity: Gating by inhibition. *Frontiers in Human Neuroscience, 4*(186), 1-8. DOI: 10.3389/fnhum.2010.00186

Kinsbourne, M. (2013). *Orientational bias model of unilateral neglect: evidence form attentional gradients within hemispace.* Psychology Press. 9780203765258

Klimesch, W. (1999). EEG alpha and theta oscillations reflect cognitive and memory performance: a review and analysis. *Brain Research Reviews, 29*(2-3), 169-195. DOI: 10.1016/S0165-0173(98)00056-3

Klimesch, W. (2012). Alpha-band oscillations, attention, and controlled access to stored information. *Trends in Cognitive Science, 16*(12), 606-617. DOI: 10.1016/j.tics.2012.10.007

Knight, R. T., Scabini, D., & Woods, D. L. (1989). Prefrontal cortex gaiting of auditory transmission in humans. *Brain Research, 504*(2), 338-342. DOI: 10.1016/0006-8993(89)91381-4

Levy, J., Heller, W., Banich, M. T., & Burton, L. A. (1983). Are variations among right-handed individuals in perceptual asymmetries caused by characteristic arousal differences between hemispheres? *Experimental Psychology: Human Perception and Performance, 9*(3), 329-359- DOI: 10.1037/0096-1523.9.3.329

Linkenkaer-Hansen, K., Nikulin, V. V., Palva, S., Ilmoniemi, R. J., & Palva, J. M. (2004). Prestimulus Oscillations Enhance Psychophysical Performance in Humans. *Journal of Neuroscience, 24*(45), 10186-10190. DOI: 10.1523/JNEUROSCI.2584-04.2004

Lotte, F., Bougrain, L., & Clerc, M. (2015). Electroencephalography (EEG)- Based Brain-Computer Interfaces. *Wiley Encyclopedia of Electrical and Electronics Engineering*, 1-44. DOI: 10.1002/047134608X.W8278

Luck, S. J., & Gaspelin, N. (2016). How to get statistically significant effects in any ERP experiment (and why you shouldn't). *Psychophysiology, 54*(1), 146–157. DOI: 10.1111/psyp.12639

Luck, S. J., Hillyard, S. A., Mangun, G. R., & Gazzaniga, M. S. (1994). Independent Attentional Scanning in the Separated Hemispheres of Split-Brain Patients. *Journal of Cognitive Neuroscience, 6*(1), 84-91. DOI: 10.1162/jocn.1994.6.1.84

Mathewson, K. E., Lleras, A., Beck, D. M., Fabiani, M., Ro, T., & Gratton, G. (2011). Pulsed out of awareness: EEG alpha oscillations represent a pulsed-inhibition of ongoing cortical processing. *Frontiers in Psychology, 2*(99), 1-15. DOI: 10.3389/fpsyg.2011.00099

Palva, S., Linkenkaer-Hansen, K., Näätänen, R., & Palva, J. M. (2005). Early Neural Correlates of Conscious Somatosensory Perception. *Journal of Neuroscience, 25*(21), 5248-5258. DOI: 10.1523/JNEUROSCI.0141-05.2005

Perrin, F., Pernier, J., Bertrand, O., & Echallier, J. F. (1989). Spherical splines for scalp potential and current density mapping. *Electroencephalography and Clinical Neurophysiology, 72*(2), 184-187. DOI: 10.1016/0013-4694(89)90180-6

Pessoa, L., Kastner, S., & Ungerleider, L. G. (2003). Neuroimaging Studies of Attention: From Modulation of Sensory Processing to Top-Down Control. *Journal of Neuroscience, 23*(10), 3990-3998. DOI: 10.1523/JNEUROSCI.23-10-03990.2003

Rajagovindan, R: & Ding, M. (2011). From Prestimulus Alpha Oscillation to Visual-evoked Response: An Inverted-U Function and its Attentional Modulation. *Journal of Cognitive Neuroscience, 23*(6), 1379-1394. DOI: 10.1162/jocn.2010.21478

RStudio Team (2022). *RStudio: Integrated Development for R. RStudio*. PBC. http://www.rstudio.com/

Stam, C. J., Nolte, G., & Daffertshofer, A. (2007). Phase lag index: Assessment of functional connectivity from multi channel EEG and MEG with diminished bias from common sources. *Human Brain Mapping, 28*(11), 1178-1198. DOI: 10.1002/hbm.20346

Thut, G., Nietzel, A., Brandt, S. A., & Pascual-Leone, A. (2006). α-Band Electroencephalographic Activity over Occipital Cortex Indexes Visuospatial Attention Bias and Predicts Visual Target Detection. *Journal of Neuroscience, 26*(37), 9494-9502. DOI: 10.1523/JNEUROSCI.0875-06.2006

Tomasi, D. & Volkow, N. D. (2012). Abnormal Functional Connectivity in Children with Attention-Deficit/Hyperactivity Disorder. *Biological Psychiatry, 71*(5), 443-450. DOI: 10.1016/j.biopsych.2011.11.003

Van der Lubbe, R. H. J., Blom, J. H. G., De Kleine, E., & Bohlmeijer, E T. (2017). Comparing the effects of sustained and transient spatial attention on the orienting towards and the processing of eletrical nociceptive stimuli. *International Journal of Psychology, 112*(), 9-21. DOI: 10.1016/j.ijpsycho.2016.11.015

Wang, C., Rajagovindan, R., Han, S. M., & Ding, M. (2016). Top-down control of visual alpha oscillations: Sources of control signals and their mechanisms of action. *Frontiers in Human Neuroscience, 10(*15), 1-14. DOI: 10.3389/fnhum.2016.00015

Weiss, S. M., Meltzoff, A. N., & Marshall, P. J. (2018). Neural measures of anticipatory bodily attention in children: Relations with executive function. *Developmental Cognitive Neuroscience, 34*(), 148-158. DOI: 10.1016/j.dcn.2018.08.002

Weisz, N., Wühle, A., Monittola, G., Demarchi, G., Frey, J., Popov, T., & Braun, C. (2014). Prestimulus oscillatory power and connectivity patterns predispose conscious somatosensory perception. *Proceedings of the National Academy of Sciences, 111*(4), 417-425. DOI: 10.1073/pnas.1317267111

Whitmarsh, S., Oostenveld, R., Almeida, R., & Lundqvist, D. (2017). Metacognition of attention during tactile discrimination. *Neuroimage, 147()*, 121-129. DOI: 10.1016/j.neuroimage.2016.11.070

Wright, T. J., Roque, N. A., Boot, W. R., & Stothart, C. (2018). Attention capture, processing speed, and inattentional blindness. *Acta Psychologica, 190*(), 72-77. DOI: 10.1016/j.actpsy.2018.07.005

Yamaguchi, S. & Knight, R. T. (1990). Gating of somatosensory input by human prefrontal cortex. *Brain Research, 521*(1-2), 281-288. DOI: 10.1016/0006-8993(90)91553-S

A. Appendix

Appendix A.

Programming Code in Python

Python Packages needed for Analysis

```
import os
import pickle
from glob import glob
import numpy as np
import mne
from mne.event import define_target_events
from mne.preprocessing import ICA, create_eog_epochs
from mne.connectivity import spectral_connectivity
from mne.viz import plot_sensors_connectivity
from pyvista import BackgroundPlotter
import sys
numpy.set_printoptions(threshold=sys.maxsize)
```

Import Data Files

```
#give file (individual) a name + save (path of file and saving directory)
File_name = r'data path'
ica_dir = r'saving directory path'
raw = mne.io.read_raw_brainvision(File_name, preload = True)
raw.info.get('nchan')#number of channels
raw.plot()#plot raw data
```

Set Montage

```
#fit headshape by digitization of montage + give channel the right type (=eeg)
raw.pick_types (meg=False, eeg=True, eog=True, ecg=False, emg=True)
raw.set_channel_types(mapping={'vEOG' : 'eog'})#ocular signals
raw.set_channel_types(mapping={'hEOG' : 'eog'})#ocular signals
raw.set_channel_types(mapping={'LEMG' : 'emg'})#muscular signals
raw.set_channel_types(mapping={'REMG' : 'emg'})#muscular signals
montage = mne.channels.make_standard_montage('standard_1020')
raw.set_montage(montage)
```

Marking of Bad Channels & Interpolation

raw.info['bads'] += []#*manually enter bad channels*

raw.interpolate_bads()#*clears out raw.info['bads'] after interpolations so that the interpolated channels are no longer excluded from subsequent computations*

Band-Pass Filter & Independent Component Analysis

raw = raw.filter(0.1, 30)#*band-pass filtering in the range 0.1Hz to 30Hz*

#Setting up ICA:

ica = mne.preprocessing.ICA()#*default setting: (n_components=None, *, max_pca_components=None, n_pca_components=None, noise_cov=None, random_state=None, method='fastica', fit_params=None, max_iter=200, allow_ref_meg=False, verbose=None)*

#Additional Info:

#1) n components = None: => number of pca components (deprecated) or 0.999999 will be used, whichever results in fewer components

#2) random state = None: => seed will be obtained from the operating system

ica.fit(raw)#*proceeds in two steps: 1) Whitening the data by means of a pre-whitening step (here:SD of each channel type) followed by PCA*
2) Passing the n_components largest-variance components to the ICA algorithm to obtain the unmixing matrix

eog_indices, eog_scores = ica.find_bads_eog(raw, 'vEOG')#*automatically find the ICs that best match the EOG signal*

ica.exclude = eog_indices#*excludes artefacts matching eog signals*

ica.plot_scores(eog_scores) #*barpolt of ICA component "EOG" match scores*

ica.plot_properties(raw, picks=eog_indices) # *plot diagnostics*

ica.plot_sources(raw, show_scrollbars=True) # *plot ICs applied to raw data, with EOG matches highlighted*

ica.exclude = [ ]#*exclude additional ICA components*

reconst_data = raw.copy()

ica.apply(reconst_data)#*proceeds in 4 steps: 1)Unmixes the data with the unmixing matrix*
 # 2)Includes ICA components based on ica.exclude
 # 3)Re-mixes the data with mixing_matrix

 # 4)Restores any data not passed to the ICA algorithm (i.e. PCA components between n_components & n_pca_components)

Save Cleaned Data File

reconst_data.save(r'save directory path.fif')

Create Event Markers

#create event markers for epochs to be formed around

events, _ = mne.events_from_annotations(raw, event_id={'Stimulus/S701': 701, 'Stimulus/S801': 801,
'Stimulus/S702': 702, 'Stimulus/S802': 802,
'Stimulus/S703': 703, 'Stimulus/S803': 803,
'Stimulus/S704': 704, 'Stimulus/S804': 804,
'Stimulus/S705': 705, 'Stimulus/S805': 805,
'Stimulus/S706': 706, 'Stimulus/S806': 806,
'Stimulus/S707': 707, 'Stimulus/S807': 807,
'Stimulus/S708': 708, 'Stimulus/S808': 808,})

event_dict = {'Sustained/Cued/Low/Left': 701, 'Sustained/Uncued/Low/Left': 801,
'Transient/Cued/Low/Left': 702, 'Transient/Uncued/Low/Left': 802,
'Sustained/Cued/Low/Right': 703, 'Sustained/Uncued/Low/Right': 803,
'Transient/Cued/Low/Right': 704, 'Transient/Uncued/Low/Right': 804,
'Sustained/Cued/High/Left': 705, 'Sustained/Uncued/High/Left': 805,
'Transient/Cued/High/Left': 706, 'Transient/Uncued/High/Left': 806,
'Sustained/Cued/High/Right': 707, 'Sustained/Uncued/High/Right': 807,
'Transient/Cued/High/Right': 708, 'Transient/Uncued/High/Right': 808}

#create plot showing at what times selected stimuli are

fig = mne.viz.plot_events(events, event_id=event_dict, sfreq=raw.info['sfreq'])

fig.subplots_adjust(right=0.6)*#to make room for legend(description)<- smaller number bigger legend*

Create Epochs & Drop Bad Epochs

#setting maximum & minimum acceptable peak-to-peak amplitudes for each channel type in each epoch created

#set start time and end time of the epoch around event marker

#set baseline

```
reject_criteria = dict(eeg=100e-6) #100uV(maximum peak-to-peak amplitude)
flat_criteria = dict(eeg=1e-6)#1uV(minimum peak-to-peak amplitude)
tmin, tmax = -1.25, 0 #epoch time window (from -1250ms till 0ms relative to nociceptive stimulus onset)
baseline = -1.25, -1 #from -1250ms till -1000ms relative to nociceptive stimulus onset
#create epochs
epochs = mne.Epochs(raw, events, event_id=event_dict,
        tmin=tmin, tmax=tmax, baseline=baseline,
        reject=reject_criteria, flat=flat_criteria,
        reject_by_annotation=True, preload=True)
print(epochs.drop_log)#print all dropped epochs including responsible channel
epochs.plot_drop_log()#graphic showing dropped epochs & shows the channels that caused the dropping
#Additional Information:
#epochs not dropped yet, however, marked!
#drop epochs later IF reject and/or flat criteria have already been provided by:
epochs.drop_bad()#drop bad epochs
print(epochs)#check if epochs have in fact been dropped
print(epochs['Transient'])#print remaining good transient epochs
print(epochs['Sustained'])#print remaining good sustained epochs
#graphic of all transient & sustained epochs (print 5 epochs per section)
epochs['Transient'].plot(events=events, event_id=event_dict, n_epochs=5)
epochs['Sustained'].plot(events=events, event_id=event_dict, n_epochs=5)
#save epochs
epochs['Transient'].save(r'save directory.fif')
epochs['Sustained'].save(r' save directory.fif')
```

Sensor-Level Spectral Connectivity

```
##necessary steps only for average of all participants
#create list object for all sustained epochs & transient epcohs
list_epochs_1 = [sus_epochs_1, sus_epochs_2, sus_epochs_3, sus_epochs_4, sus_epochs_5,
      sus_epochs_6, sus_epochs_7, sus_epochs_8, sus_epochs_9, sus_epochs_10,
      sus_epochs_11, sus_epochs_12, sus_epochs_13, sus_epochs_14, sus_epochs_15]
list_epochs_2 = [tra_epochs_1, tra_epochs_2, tra_epochs_3, tra_epochs_4, tra_epochs_5,
```

```
        tra_epochs_6, tra_epochs_7, tra_epochs_8, tra_epochs_9, tra_epochs_10,
        tra_epochs_11, tra_epochs_12, tra_epochs_13, tra_epochs_14, tra_epochs_15]
#create object with all epochs included
epochs_1 = mne.concatenate_epochs(epochs_list=list_epochs_1)
epochs_2 = mne.concatenate_epochs(epochs_list=list_epochs_2)


#Compute Connectivity
#use of PLI method and multitaper with 7 DPSS windows
#sustained attention
picks = mne.pick_types(epochs_1.info, eeg=True, meg=False, stim=False, eog=False)
fmin, fmax = 8., 13.#define frequency band (alpha-mu: 8-13Hz, beta: 14-30Hz)
sfreq = epochs_1.info['sfreq']#determine the sampling frequency
tmin = -1#remove baseline
#compute connectivity for left hand
epochs_1.load_data().pick_types(eeg=True)#just keep EEG and no EOG now
con, freqs, times, n_epochs, n_tapers = spectral_connectivity(
   epochs_1[‘Left’], method='pli', mode='multitaper', sfreq=sfreq, fmin=fmin, fmax=fmax,
   faverage=True, tmin=tmin, mt_adaptive=False, n_jobs=1)
plot_sensors_connectivity(epochs_1.info, con[:, :, 0])#create graph
#compute connectivity for right hand
epochs_1.load_data().pick_types(eeg=True)#just keep EEG and no EOG now
con, freqs, times, n_epochs, n_tapers = spectral_connectivity(
   epochs_1[‘Right’], method='pli', mode='multitaper', sfreq=sfreq, fmin=fmin, fmax=fmax,
   faverage=True, tmin=tmin, mt_adaptive=False, n_jobs=1)
plot_sensors_connectivity(epochs_1.info, con[:, :, 0])#create graph

#transient attention
picks = mne.pick_types(epochs_2.info, eeg=True, meg=False, stim=False, eog=False)
fmin, fmax = 8., 13. #define frequency band (alpha-mu: 8-13Hz, beta: 14-30Hz)
sfreq = epochs_2.info['sfreq'] #determine the sampling frequency
tmin = -1#remove baseline
#compute connectivity for left hand
epochs_2.load_data().pick_types(eeg=True)#just keep EEG and no EOG now
con, freqs, times, n_epochs, n_tapers = spectral_connectivity(
```

~~~
    epochs_2[‘Left’], method='pli', mode='multitaper', sfreq=sfreq, fmin=fmin, fmax=fmax,
    faverage=True, tmin=tmin, mt_adaptive=False, n_jobs=1)
plot_sensors_connectivity(epochs_2.info, con[:, :, 0]) #create graph
#compute connectivity for right hand
epochs_2.load_data().pick_types(eeg=True)#just keep EEG and no EOG now
con, freqs, times, n_epochs, n_tapers = spectral_connectivity(
    epochs_2[‘Right’], method='pli', mode='multitaper', sfreq=sfreq, fmin=fmin, fmax=fmax,
    faverage=True, tmin=tmin, mt_adaptive=False, n_jobs=1)
plot_sensors_connectivity(epochs_2.info, con[:, :, 0]) #create graph
~~~

Appendix B

R-code used for the multi-factorial linear analysis and model acceptance

~~~
#packages needed for analysis
```{r setup, include=FALSE}
knitr::opts_chunk$set(echo = TRUE)
```
`````{r eval=FALSE, include=FALSE}
install.packages("remotes")
remotes::install_github("schmettow/bayr")
devtools::install_github("schmettow/bayr")
```
```{r}
library("readxl")
library(tidyverse)
library(rstanarm)
library(mascutils)
library(brms)
library(bayr)
options(mc.cores = 4)
```
#load data
```{r}
my_data <- read_excel("C:/Users/User/Desktop/Master Thesis/Tables/R_table.xlsx")
```
~~~

````
#run analysis + create Table with data
```{r}
M_3_la <-
my_data %>%
brm(Connectivity ~ Condition + Hand + Sensor + Condition:Hand + Condition:Sensor +
Hand:Sensor,
family = Beta(link = "logit"),
data = .)
```
```{r}
fixef_ml (M_3_la)
```
#check for model acceptance
```{r}
bind_rows(
  posterior(M_2_la),
  posterior(M_3_la)) %>%
coef() %>%
ggplot(aes(y = parameter, col = model,
           xmin = lower, xmax = upper, x = center)) +
geom_crossbar(position = "dodge") +
labs(x = "effect")
```
````

Appendix C

Pre-processed Analysis Details

(-1.25 – 0(baseline: -1.25--1):

Not more than 15% of Epochs allowed to drop

Participant (Nr.)	Interpolated Channels	Excluded ICA components	Dropped Epochs of each condition	Total of dropped Epochs
16 (Age:20, Female, Lefthanded)				EXCLUDED AS DATA NOT SUFFICIENT
10(sustained) 10(transient) (Age:25, Female, Right)	AF8 AF8	0, 1, 37 0, 1	0 out of 192 0 out of 192	0 out of 384
12(sustained) 12(transient) (Age:22, Female, Righthanded)	T7, T8, TP8 T7, T8, TP8	2, 6, 31 0, 4	2 out of 192 5 out of 192	7 out of 384
21 (Age: 22, Male, Righthanded)				EXCLUDED AS DATA NOT SUFFICIENT
14(transient) 14(sustained) (Age:23, Female, Righthanded)	F7, F5, FC5 F7, F5, FC5	0, 1, 2 0, 1	0 out of 192 2 out of 192	2 out of 384
22(transient) 22(sustained) (Age:25, Male, Righthanded)	FT7, T7 FT7, T7	0, 1 1, 2	3 out of 192 1 out of 192	4 out of 384
26 (Age:23, Female, Righthanded)	None	0, 1	Sustained:8 out of 192 Transient:11 out	19 out of 384

			of 192	
18(sustained) 18(transient) (Age:23, Female, Righthanded)	None None	0, 1 0, 1, 29	2 out of 192 4 out of 192	6 out of 384
13 (Age:24, Female, Righthanded)	Fp2, TP8	0,1	Sustained: 0 out of 192 Transient: 0 out of 191	0 out of 383
17 (Age:22, Female, Righthanded)	T7	0, 1, 59	Sustained: 11 out of 192 Transient: 0 out of 191	11 out of 383
23 (Age:23, Male, Righthanded)	AF8	0, 2	Sustained: 0 out of 192 Transient: 1 out of 192	1 out of 384
11 (Age:31, Female, Righthanded)	FC5, AF3, T7, P8	0, 1	Sustained: 2 out of 192 Transient: 1 out of 192	3 out of 384
19 (Age:22, Female, Righthanded)	T8	2	Sustained: 4 out of 192 Transient 34 out of 192	38 out of 384
20(sustained) 20(transient) (Age:26, Female, Righthanded)	T7 T7	0, 1, 2 0, 1, 5	0 out of 192 1 out of 192	1 out of 384
24(transient) 24(sustained) (Age:22, Female, Righthanded)	T8 T8	1, 2, 18 2, 4	1 out of 192 2 out of 192	3 out of 384
15 (Age: 22, Female,	AF8, F7, T7	0, 1, 28	Sustained: 0 out of 192 Transient: 0 out	0 out of 384

Righthanded			of 192	
25 (Age:34, Female, Righthanded)	None	0, 1, 49	Sustained: 0 out of 192 Transient: 0 out of 190	0 out of 382

Appendix D

Descriptive statistics of the connectivity means and standard deviation & results of two-way ANOVA

Table 3

Descriptive statistics of the connectivity means and standard deviation within the alpha-mu frequency between electrode pairs AF3-CP3 and AF4-CP4 divided by the Side Factor (left sided or right sided) and condition (sustained tactile attention or transient tactile attention)

Sensor Pairs	***Condition***	***Mean***	***Std. Deviation***
AF3/CP3 Left Hand	Sustained	.126	.082
	Transient	.139	.105
AF4/CP4 Left Hand	Sustained	.124	.065
	Transient	.127	.063
AF3/CP3 Right Hand	Sustained	.135	.079
	Transient	.119	.080
AF4/CP4 Right Hand	Sustained	.153	.076
	Transient	.142	.100

Note: Results for electrode pair x condition, $F(1, 12) = .006$, $p = .942$, results for electrode pair x condition x side, $F(1, 12) = .135$, $p = .720$, results for side x electrode pair $F(1, 12) = 1.141$, $p = .307$. None of the interaction appears significant.

Table 4

Descriptive statistics of the connectivity means and standard deviation within the beta frequency between electrode pairs AF3-CP3 and AF4-CP4 divided by the Side Factor (left sided or right sided) and condition (sustained tactile attention or transient tactile attention)

Sensor Pairs	***Condition***	***Mean***	***Std. Deviation***
AF3/CP3 Left Hand	Sustained	.112	.041
	Transient	.103	.027
AF4/CP4 Left Hand	Sustained	.090	.017
	Transient	.095	.025
AF3/CP3 Right Hand	Sustained	.099	.028
	Transient	.098	.035
AF4/CP4 Right Hand	Sustained	.095	.022
	Transient	.089	.032

Note: Results for electrode pair x condition, $F(1, 10) = .115$, $p = .742$, results for electrode pair x condition x side, $F(1, 10) = .1983$, $p = .189$, results for side x electrode pair with $F(1, 10) = .441$, $p = .552$. None of the interaction appears significant.

Appendix E

Model Acceptance Graphs

For alpha-mu:

For beta:

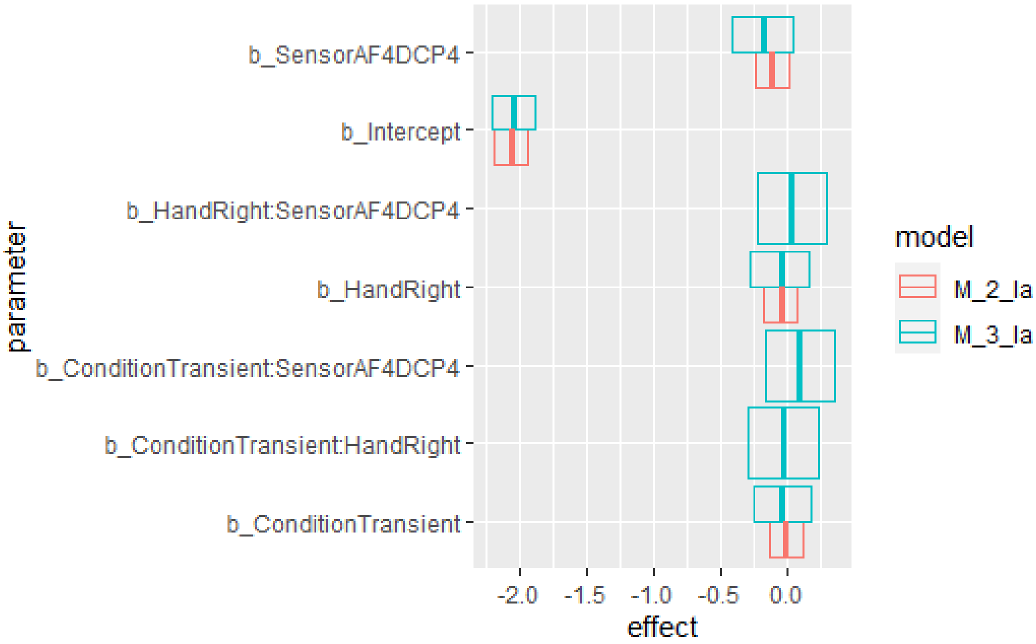
b_SensorAF4DCP4
b_Intercept
b_HandRight:SensorAF4DCP4
b_HandRight
b_ConditionTransient:SensorAF4DCP4
b_ConditionTransient:HandRight
b_ConditionTransient
parameter
-2.0
-1.5
-1.0
-0.5
0.0
effect
model
M_2_la
M_3_la